

Multiple Localized States and Magnetic Orderings in Partially Open Zigzag Carbon Nanotube Superlattices: An Ab Initio Study

Bing Huang^{1,2}, Zuanyi Li³, Young-Woo Son⁴, Gunn Kim^{5*}, Wenhui Duan^{1†}, and Jisoon Ihm²

¹ *Department of Physics, Tsinghua University,
Beijing 100084, People's Republic of China*

² *FPRD and Department of Physics and Astronomy,
Seoul National University, Seoul 151-747, Republic of Korea*

³ *Department of Physics, University of Illinois at
Urbana-Champaign, Urbana, Illinois 61801-3080, USA*

⁴ *Korea Institute for Advanced Study, Seoul 130-722, Republic of Korea*

⁵ *Department of Physics, Kyung Hee University, Seoul 130-701, Korea*

(Dated: September 5, 2018)

Abstract

Using ab initio calculations, we examine the electronic and magnetic properties of partially open (unzipped) zigzag carbon nanotube (CNT) superlattices. It is found that depending on their opening degree, these superlattices can exhibit multiple localized states around the Fermi energy. More importantly, some electronic states confined in some parts of the structure even have special magnetic orderings. We demonstrate that, as a proof of principle, some partially open zigzag CNT superlattices are by themselves giant (100%) magnetoresistive devices. Furthermore, the localized (and spin-polarized) states as well as the band gaps of the superlattices could be further modulated by external electric fields perpendicular to the tube axis, and a bias voltage along the tube axis may be used to control the conductance of two spin states. We believe that these results will open the way to the production of novel nano-scale electronic and spintronic devices.

* gunnkim@khu.ac.kr

† dwh@phys.tsinghua.edu.cn

I. INTRODUCTION

Low dimensional sp^2 -bonded carbon materials have attracted tremendous attention because of their unique electronic properties and potential applications in nano-scale devices.¹⁻⁴ For examples, depending on their diameters and chiralities, carbon nanotubes (CNTs) can be either metallic or semiconducting, and the later ones (*e.g.*, semiconducting zigzag CNTs) are suitable for making nano-scale electronic devices.³⁻⁶ Graphene nanoribbons (GNRs), which could be regarded as unrolled CNTs, also exhibit unique electronic structures strongly dependent on the orientation of their edges and width.⁷⁻¹⁰ On the other hand, superlattices as well as various quantum structures based on CNTs or GNRs have been the subject of active research in the past decades, and one-dimensional quantum wells and zero-dimensional quantum dots have been shown to form by either CNT-based¹¹⁻¹⁶ or GNR-based¹⁷⁻²⁵ structures.

So far, most studies of CNTs and GNRs have been conducted independently. The experimental realization of GNRs generally relies on standard e-beam (or microscope) lithography,²⁶⁻²⁸ chemical method,²⁹ or synthetic method.³⁰ Quite recently, however, several promising methods were developed by using CNTs to fabricate GNRs or CNT-GNR junctions via longitudinal cutting³¹⁻³⁸ such as chemical attack or plasma etching to unzip CNTs.^{31-33,36,37} Besides, the side wall of CNTs can be opened longitudinally by intercalation of lithium atoms or transition metal clusters and then ammonia followed by exfoliation.^{34,35} More interestingly, the degree of stepwise opening in CNTs can be controlled by the experimental conditions, such as the amount of oxidizing agents, lithium atoms, or transition metal clusters, and partially open (unzipped) CNTs (or CNT-GNR junctions) have been observed in transmission electron microscopy images.^{31,32,34-37} These experimental progresses imply that CNTs and GNRs can be combined together with perfect-atomic-interfaces and new superlattices with CNT-GNR junctions can be realized.^{31,32,34-37} In such nanostructures, the openings of CNTs (*i.e.*, curved GNR parts) would offer various edges which are suitable for doping, adsorption, and chemical functionalization. In particular, zigzag edges have been found to exhibit localized edge states and unique magnetic ordering in GNRs and graphene nanostructures.^{10,18-22,39,40} Being composed of both a CNT and a curved GNR (with plenty edge structures), a partially open CNT is therefore expected to have more diverse electronic and magnetic properties than a pristine CNT or GNR, and these properties may be

sensitively dependent on the opening degree.

Previous theoretical works only focused on partially open (unzipped) *armchair* CNTs and demonstrated that they are by themselves magnetoresistive⁴¹ and spin-filter devices.^{42,43} In contrast, as far as we know, the physical properties of partially open *zigzag* CNTs have been poorly investigated until now. In this work, electronic and magnetic properties of superlattices made of partially open zigzag CNTs are investigated using spin-polarized density functional theory (DFT) calculations. Depending on the opening degree, the superlattices are found to show semiconducting or spin-polarized semiconducting/metallic behaviors. Besides, some localized states appear around the Fermi level and some of them could serve as quantum well states which cannot be achieved in partially open armchair CNTs. Especially, magnetic (spin) ordering can be realized in these superlattice structures and mainly depends on the opening width rather than length unlike partially open armchair CNTs. Our calculations further suggest some special partially open zigzag CNTs superlattices can also act as giant magnetoresistive devices under magnetic fields. Furthermore, the band gap as well as the localized states could be modulated by external transverse electric fields, and the conductance of two spin states may be tuned by a bias voltage along the tube axis.

II. COMPUTATIONAL METHODS AND MODELS

We carried out electronic structure calculations using the projector augmented wave (PAW) potentials⁴⁴ and the generalized gradient approximation (GGA) with the Perdew-Burk-Ernzerhof (PBE) functional⁴⁵ implemented in the Vienna *Ab initio* Simulation Package (VASP).⁴⁶ The energy cutoff for a plane wave basis set is 400 eV. Our models are optimized until energies are converged to 10^{-5} eV and atomic forces are smaller than 0.02 eV/Å. The supercell is sufficient large to ensure that the vacuum space between the adjacent CNTs are at least 10 Å to avoid the interaction. Three Monkhost-Pack k -point meshes are employed, yielding an ~ 1 meV per atom convergence of the total energy. The optimized geometrical structures are used to calculate the electronic and magnetic structures under uniform external electric field (E_{ext}), implemented using a dipole layer in the vacuum as in the work of Neugebauer and Scheffler.⁴⁷

Before the discussion of our models and results, we first introduce the definition of partially open CNT superlattices following the convention of previous work.⁴² As shown in

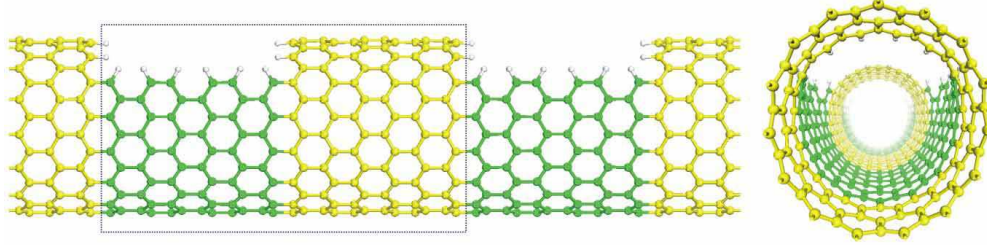


FIG. 1: Structures of partially open (n, m) CNTs, $\text{NT}(n, m, L_t)\text{-ONT}(W, L_o)$. Yellow and green balls represent carbon atoms on the perfect CNT and the open CNT parts, respectively. The openings are terminated with hydrogen atoms, represented by small white balls. The rectangle marks one supercell of partially open CNTs. This figure shows the structure of $\text{NT}(15, 0, 6)\text{-ONT}(4, 6)$ representing a partially open $(15, 0)$ CNT which has 6 (6) C-C dimer lines in the perfect CNT part (open part) along the tube axis, and the missing rows in the opening is 4.

Figure 1, a partially open CNT consists of two parts: a perfect CNT part (yellow color) and an opening (green color). We represent the system as $\text{NT}(n, m, L_t)\text{-ONT}(W, L_o)$ where n and m correspond to the chiral vector of the CNT, L_t (L_o) is the length in the tube axis direction of the perfect (open) CNT in the units of columns of carbon atoms. W is the missing width in units of carbon rows for the opening. For example, we denote the structure (in Figure 1) as $\text{NT}(15, 0, 6)\text{-ONT}(4, 6)$. Such a supercell is repeated periodically in the tube axis direction to form a superlattice.

III. RESULTS AND DISCUSSION

A zigzag CNT could be either semiconducting or almost metallic at room temperature.³ Thus, it is expected that partially open CNTs obtained from distinct zigzag CNTs may show different features depending on their chiralities. The $(13, 0)$ CNT (with a band gap of ~ 0.72 eV in our calculations) and the $(15, 0)$ CNT (with a band gap of ~ 0.04 eV) are considered to construct superlattices. We find that the electronic properties, especially the magnetic properties, of both kinds of partially open zigzag CNT superlattices depend more sensitively on the cutting width than the cutting length; this is evidently different from the partially open armchair CNTs.⁴¹⁻⁴³ Furthermore, for both $(13, 0)$ and $(15, 0)$ CNTs, the spin-polarization takes place at the discontinuous zigzag edges of the opening when the cutting width $W > 5$. Two different cutting widths ($W = 4$ and $W = 6$) are chosen to

TABLE I: The relation between the energy band gap E_g (eV) and the cutting length L_o of partially open (13, 0) and (15, 0) CNT superlattices for two different cutting width (W) [$L_t + L_o = 12$]. As in $W = 6$ case, the energy differences ΔE (eV/cell) between antiferromagnetic (AFM) ground states and nonmagnetic (NM) states are also shown.

NT(13, 0, L_t)-ONT (W, L_o)				NT(15, 0, L_t)-ONT (W, L_o)			
E_g	$L_o = 4$	$L_o = 6$	$L_o = 8$	E_g	$L_o = 4$	$L_o = 6$	$L_o = 8$
$W = 4$ (NM)	0.330	0.295	0.224	$W = 4$ (NM)	0.321	0.365	0.384
(AFM)	0.458	0.462	0.475	(AFM)	0.193	0.189	0.174
$W = 6$				$W = 6$			
ΔE	-0.164	-0.135	-0.064	ΔE	-0.057	-0.043	-0.020

represent nonmagnetic (NM) and spin-polarized system, respectively. In the following, we keep the total length of the superlattices as 2.56 nm ($L_t + L_o = 12$), and then change the cutting length L_o . The results are listed in Table I.

For $W = 4$, the overall geometric structures change slightly when the cutting length is short. As the cutting length becomes longer, the middle part of the opening is widened to release the compressive stress and lower the total energy, which is similar to partially open armchair CNTs^{41–43,48} and agrees with experimental observations.^{31,32,34–37} The partially open (13, 0) and (15, 0) CNT superlattices are still semiconductors without any magnetic ordering. However, their band gaps change much compared with perfect (15, 0) and (13, 0) CNTs, as listed in Table I.

As an example, Figure 2 shows the electronic properties of NT(13, 0, 6)-ONT(4, 6) and NT(15, 0, 6)-ONT(4, 6) superlattices. The band structures of perfect (13, 0) and (15, 0) CNTs, which are calculated in the supercell six times than the primitive unit cell, are also displayed in the left panels of Figs. 2b and 2e for comparison. The bands around the Fermi level of perfect (13, 0) and (15, 0) CNTs are doubly-degenerate, but the degeneracy disappears due to cylindrical symmetry breaking. This is evident from the increased numbers of visible bands in the right panels of Figs. 2b and 2e. Two bands with small dispersions arise around the Fermi level in the NT(13, 0, 6)-ONT(4, 6) superlattice, and consequently, the band gap of NT(13, 0, 6)-ONT(4, 6) is $\sim 50\%$ smaller than that of the perfect one. Charge density analysis (Figure 2c) shows that most of charge densities of the two bands

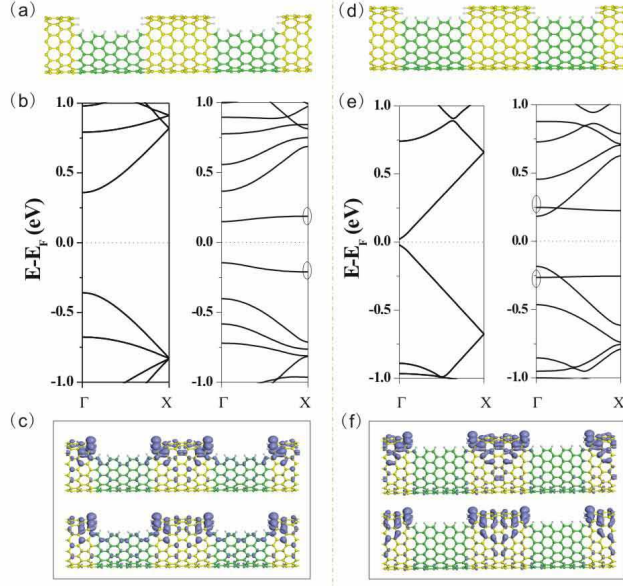


FIG. 2: (a) The optimized structure of NT(13, 0, 6)-ONT(4, 6) superlattice (side view). (b) From left to right, the band structures of the perfect (13, 0) CNT with six times primitive unit cell and NT(13, 0, 6)-ONT(4, 6) superlattice. (c) Side view of the charge density on the top valence band (upper figure) and the bottom conduction band (lower figure) at the X-point of the band structure in (b)(marked with circles). (d) The optimized structure of NT(15, 0, 6)-ONT(4, 6) superlattice (side view). (e) From left to right, the band structures of perfect (15, 0) CNT with six times primitive unit cell and NT(15, 0, 6)-ONT(4, 6) superlattice. (f) Side view of the charge density on the top valence band (upper figure) and the bottom conduction band (lower figure) at the Γ -point of the band structure in (e)(marked with circles). The Fermi level is set to zero.

are located at the top of the perfect CNT part (especially located at the zigzag edges) and contributed mainly by the p_z orbitals of carbon atoms. The physical origin of these localized states is similar to that of zigzag graphene nanoribbons (ZGNRs). Previous works show that the zigzag edges of graphene (or ZGNRs) induce localized edge states around the Fermi level.^{7-9,39,49} As the cutting length L_o increases from 4 to 8, the energy differences between the two localized states (*i.e.*, band gap between the top valence and bottom conduction bands) decrease from 0.330 eV to 0.224 eV (Table I), and the two bands become a little more dispersive due to the hybridization with π and π^* bands (the second highest valence band and second lowest conduction band) near the Γ point. Similar to NT(13, 0, 6)-ONT(4, 6) superlattice, there are also two new flat bands located close to the top valence band and

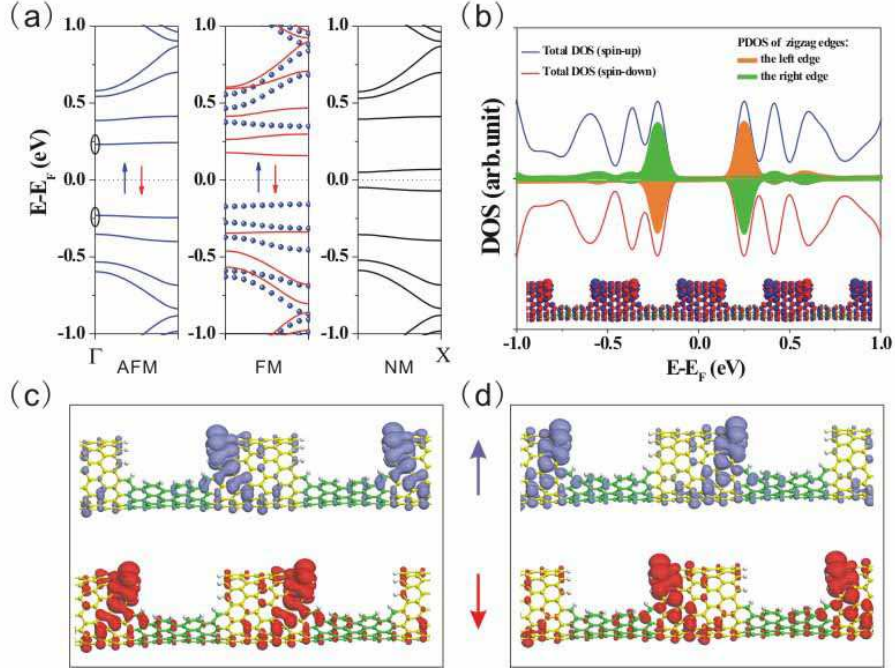


FIG. 3: (a) From left to right, the band structures of NT(13, 0, 6)-ONT(6, 6) superlattice for AFM, FM, and NM states, respectively. (b) The total density of states (DOS) of NT(13, 0, 6)-ONT(6, 6) superlattice in the AFM ground state. The partial density of states (PDOS) of two zigzag edges at the opening is also plotted as green (for right) and orange (for left) filled area under DOS curve. The spatial spin density distribution of AFM ground state is shown as inset. The Fermi level is set to zero. (c) The spin-up and -down charge densities (side views) of the top valence band at the Γ -point in the AFM state [the lower circle in (a)]. (d) The spin-up and -down charge densities (side views) of the bottom conduction band at the Γ -point in the AFM state [the upper circle in (a)]. In these figures, blue and red colors represent the spin-up and spin-down states, respectively.

the bottom conduction band for NT(15, 0, 6)-ONT(4, 6) superlattice. The two flat bands are also mainly located at the zigzag edges of the top perfect CNT part, as shown in Figure 2f. The origin of these localized states is the same as in NT(13, 0, 6)-ONT(4, 6) superlattice. When the cutting length L_o increases from 4 to 8, the band gap of partially open (15, 0) CNT superlattices increases slightly from 0.32 eV to 0.38 eV, whereas the energy difference between the two localized states increases from 0.40 eV to 0.63 eV.

The situation is much more interesting for $W = 6$. The ground state of these superlattices converts from NM to spin-polarized. There are two stable spin-polarized states, called

the AFM (ground) and FM states, similar to the case of ZGNRs.^{7,10,39,50} The AFM (FM) configuration exhibits antiferromagnetic (ferromagnetic) coupling between two zigzag edges in one opening and the ferromagnetic coupling at each zigzag edge, as shown in the inset of Figures 3b or Figure 4b. For $W = 6$, the band gap changes little with different cutting length, as listed in Table I; this is evidently different from the case of $W = 4$. It means that the energy gap opening mechanism of the spin-polarized case is different from that of the NM case, as explained in the following. The energy difference between the AFM ground states and NM states, however, decreases much as cutting length L_o increases.

Figures 3 and 4 show the electronic and magnetic properties of NT(13, 0, 6)-ONT(6, 6) and NT(15, 0, 6)-ONT(6, 6) superlattices, respectively. NT(13, 0, 6)-ONT(6, 6) superlattice has four flat bands around the Fermi level for both spin-polarized (AFM and FM) states and NM state, as shown in Figure 3a. Moreover, the top valence and bottom conduction bands of the AFM configurations are mostly confined at the zigzag edges of the opening, and behave as spin-polarized edge states, as shown in the partial density of states (PDOS) and the charge density in Figures 3b-3d. Comparison with the case of $W = 4$ indicates that long enough topological zigzag edges induce spin instability toward spin-band splitting, which agrees with previous finding on ZGNRs and CNTs.^{10,39,41-43,50} Another two flat states of each spin (the second highest valence band and the second lowest conduction band) are mainly located at the bottom of the tube, which behave as quantum well states (data not shown). As shown in Figures 3c and 3d, the oppositely oriented spin states are mostly located at the opposite (left and right) sides of open zigzag edges. Therefore, if an additional electron (hole) is introduced in this system, it will be confined at one zigzag edge of the opening with a certain spin direction. The flat bands around the Fermi level in the FM state (~ 0.025 eV/cell higher than the AFM state) have similar properties to the corresponding flat bands of the AFM state. It is also interesting that as the cutting length increases from 4 to 8, the dispersions and energies of the two flat bands associated with localized states change little but the energies of the other two flat bands associated with quantum well states change much (data not shown). Therefore, the existence of spin-polarized localized states and the band gaps of AFM ground state are insensitive to the cutting length but sensitive to the cutting width.

As shown in Figure 4, NT(15, 0, 6)-ONT(6, 6) superlattice exhibits an AFM ground state with 0.189 eV band gap, similar to NT(13, 0, 6)-ONT(6, 6). The top valence band

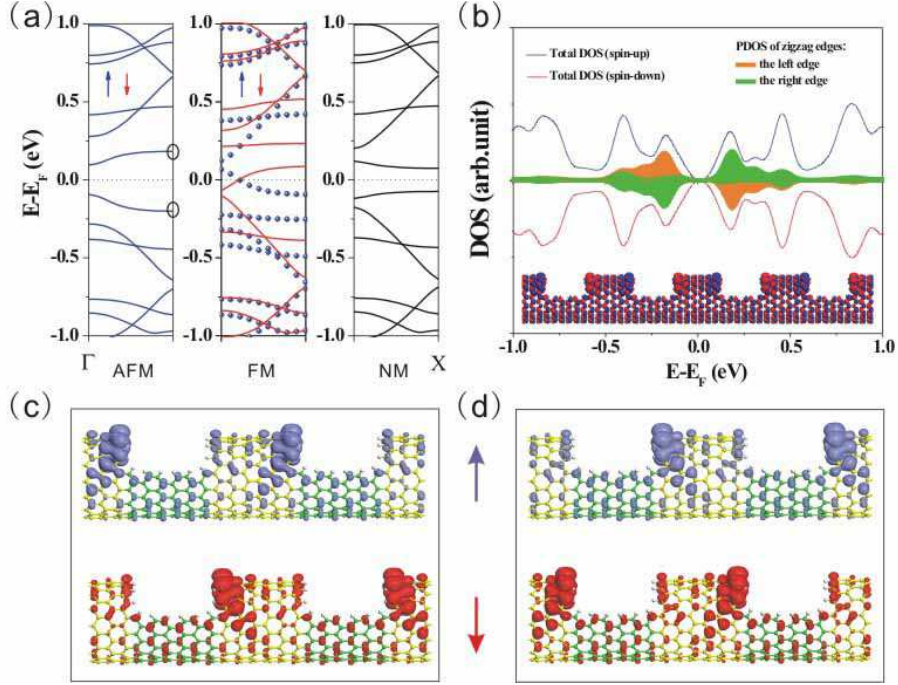


FIG. 4: (a) From left to right, the band structures of NT(15, 0, 6)-ONT(6, 6) superlattice for AFM, FM, and NM states, respectively. (b) The total DOS of NT(15, 0, 6)-ONT(6, 6) superlattice in the AFM ground state. The PDOS of two zigzag edges at opening is also plotted as green (for right) and orange (for left) filled area under DOS curve. The spatial spin density distribution of the AFM ground state is shown as inset. The Fermi level is set to zero. (c) The spin-up and -down charge densities (side views) of the top valence band at the X-point in the AFM state [the lower circle in (a)]. (d) The spin-up and -down charge densities (side views) of the bottom conduction band at the X-point in the AFM state [the upper circle in (a)]. In these figures, blue and red colors represent the spin-up and spin-down states, respectively.

and the bottom conduction band of the AFM state have a small dispersion with a flattened tail near the X-point (Figure 4a) and the charge density of the two bands at the X-point are located at the opposite (left or right) zigzag edge of the opening (Figure 4c and 4d). At the same time, the zigzag edge states are hybridized with dispersive π and π^* bands near the Γ point, as shown in Figure 4a and 4b, which is obviously different from the above NT(13, 0, 6)-ONT(6, 6) case. Unexpectedly, the FM state (~ 0.030 eV/cell higher than the AFM state) is metallic with $\sim 1.0\mu_B$ moment. As the cutting length increases from 4 to 8, the band gap of the AFM state decreases by 0.02 eV (Table I), and the FM is always metallic

TABLE II: The band gap E_g (eV) and the energy differences [ΔE (eV/cell), between AFM ground states and NM states] of NT(13, 0, L_t)-ONT(6, 6) and NT(15, 0, L_t)-ONT(6, 6) superlattices with different L_t .

NT(13, 0, L_t)-ONT (6, 6)				NT(15, 0, L_t)-ONT (6, 6)			
L_t	6	8	10	L_t	6	8	10
E_g (AFM)	0.462	0.462	0.462	E_g (AFM)	0.189	0.175	0.160
ΔE	-0.135	-0.175	-0.180	ΔE	-0.043	-0.055	-0.057

with $\sim 1.0\mu_B$ moment, independent on the cutting length. Similar results are obtained in our calculations for NT(12, 0, 6)-ONT(6, 6) superlattice, indicating that the FM states of partially open CNT superlattices made of metallic zigzag CNTs are metallic when the cutting width is large enough ($W > 5$).

In addition, we keep the opening degree ($L_o = 6$, $W = 6$) of the CNT superlattices unchanged, and then increase the total length (L_t increases as well) to study the dependence of electronic properties (especially the energy of the localized states) on L_t . The results are summarized in Table II. For NT(13, 0, L_t)-ONT(6, 6) and NT(15, 0, L_t)-ONT(6, 6) superlattices, clearly, the electronic properties (band gaps) are insensitive to the length L_t , and the overall band structure around the Fermi level retains the same for different L_t (not shown). The energy differences between the AFM state and NM states increase slightly, indicating the AFM ground state becomes a little more stable for longer L_t .

Magnetic field B can be applied to change the magnetic (spin) ordering of ZGNRs and partially unzipped armchair CNTs from the AFM configuration to FM configuration.^{41,51,52} It has been estimated that the switching B can be as low as 0.03 T at the liquid Helium temperature (4K) for ZGNRs.⁵² Similarly, it is expected that a magnetic field can also be used to turn the spin ordering of partially open zigzag CNT superlattices from AFM (ground state) configuration to FM configuration. Based on the unique electronic properties of partially open (15, 0) CNT superlattices, we propose a magnetoresistance (MR) device [a finite partially open (15, 0) CNT superlattice connected to two semi-infinite intact metallic (15, 0) CNTs], with a very large value of MR. The AFM ground state of partially open (15, 0) CNT superlattices (with $W = 6$) is semiconducting with a band gap of ~ 0.20 eV (Figure 4a), so the conductance of the AFM state around the Fermi level is zero (for an infinite

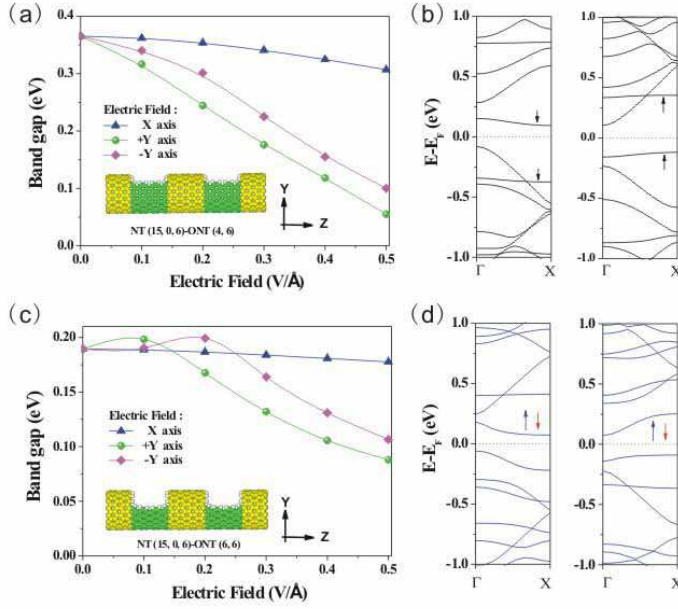


FIG. 5: Electronic properties of partially open zigzag CNT superlattices in E_{ext} . (a) The band gap as a function of E_{ext} for NT(15, 0, 6)-ONT(4, 6) superlattice. (b) From left to right, the band structures of NT(15, 0, 6)-ONT(4, 6) with $E_{\text{ext}} = 0.3 \text{ V/\AA}$ in the $+y$ and $-y$ directions, respectively. (c) The band gap as a function of E_{ext} for NT(15, 0, 6)-ONT(6, 6) superlattice. (d) From left to right, the band structures of NT(15, 0, 6)-ONT(6, 6) with $E_{\text{ext}} = 0.3 \text{ V/\AA}$ in $+y$ and $-y$ directions, respectively. The inset of (a) and (b) are the corresponding geometric structures. The Fermi level is set to zero.

superlattice) or near zero (for finite superlattice due to the coupling of the superlattice to electrodes). A sufficiently strong magnetic field B will make the superlattice ferromagnetic and hence metallic (Figure 4a), which leads to new bands (transport channels) at low energies and a finite conductance near the Fermi level. Therefore, magnetic field B can produce a dramatic change in the conductance of the system, which is quantified by the MR, defined as the relative change of the resistance when a magnetic field is applied. Based on a conventional definition of MR ($\text{MR} \equiv \frac{R_{AF} - R_{FM}}{R_{AF} + R_{FM}} = \frac{G_{FM} - G_{AF}}{G_{FM} + G_{AF}} \times 100$), we expect a $\text{MR} \sim 100\%$ can be reached in $\sim 0.20 \text{ eV}$ energy range near the Fermi level at low magnetic field B around the liquid Helium temperature.

The response of CNTs to an external transverse electric field (E_{ext}) is also of interest for its future applications.^{42,53-56} Our previous works show that the partially open armchair

CNT behaves as an electric switching or a spin-filter under an E_{ext} .^{42,43} So it is interesting to investigate the properties of partially open zigzag CNTs under E_{ext} . As an example, we have considered NT(15, 0, 6)-ONT(4, 6) and NT(15, 0, 6)-ONT(6, 6) superlattices. For convenience, all the openings in the superlattices are put in the $+y$ direction, shown as the insets of Figures 5a and 5b. The E_{ext} has been applied in three directions (x , $+y$, $-y$) perpendicular to the tube axis (z). Figure 5 briefly shows the results of the two different superlattices under E_{ext} .

For NT(15, 0, 6)-ONT(4, 6) superlattice, if E_{ext} is in the x direction, the band gap changes little (< 0.06 eV) even under 0.5 V/Å (Figure 5a). But the situation is opposite if the E_{ext} is in the $+y$ (or $-y$) direction: the band gap decreases by ~ 86 % (or ~ 72 %). Such changes in the band gap is the response of localized states to external electric fields. From the band structures of NT(15, 0, 6)-ONT(4, 6) under $E_{\text{ext}} = 0.3$ V/Å in $+y$ and $-y$ directions (Figure 5b), we can clearly see that the gap change arises from the upwards/downwards shift of the two flat bands (associated with the localized states) relative to the unperturbed bands (Figure 2e) when E_{ext} is applied in the $-y/+y$ direction. Since the two localized states are mainly composed of the p_z orbital of carbon atoms on the top part of perfect CNT, their distributions are not uniform in the y direction. Thus, E_{ext} in the y direction can effectively change the electrostatic potential of the localized states, and hence their energies. In contrast, there is no obvious difference in the x direction for these localized states (Figure 2f), so E_{ext} will not result in a net energy change of each localized state, and consequently the energy gap does not change dramatically. Our finding indicates that the energy of localized p_z orbital states could be strongly influenced by the direction of charge polarization (dipole direction) induced by E_{ext} .^{42,57} Similar changes of energy gaps are also observed in the spin-polarized NT(15, 0, 6)-ONT(6, 6) superlattice (data shown in Figures 5c and 5d) and NT(13, 0, 6)-ONT(6, 6) superlattice (data not shown here). The above discussion demonstrates that the application of E_{ext} is an effective way to control the band gap of the superlattices. Especially, the energy of the localized states can be modulated by this way for various practice purposes.

Besides the x and $\pm y$ directions, the electric field can also be applied along the tube axis (z direction). Our previous works show that if the electric field is transversely applied across the ZGNRs or partially open armchair CNTs, the occupied and unoccupied edge (localized) states associated with one spin orientation close their gap, whereas those associated with

the other spin orientation widen theirs.^{42,50,58} Then, the system can be forced into a half-metallic state by an appropriate applied electric field, resulting in an insulating behavior for one spin and metallic behavior for the other, and hence the conductance of the system becomes spin-polarized. The same idea may be applied to the partially open (15, 0) CNTs in the AFM ground state: with a bias voltage (electric field) along the tube axis (across the zigzag edges of the opening), the conductance of the two different spin states will be changed in different ways, even half-metallicity may be realized at high bias voltage.

IV. SUMMARY

In conclusion, our results obtained from ab initio calculations demonstrate that the superlattices based on partially open zigzag carbon nanotubes have interesting electronic and magnetic properties. The localized states can be formed around the top of perfect CNT parts in such superlattices and the energy gap can be modified by the size of the opening. The width of the opening determines whether the ground state of the system is spin-polarized or not. Interestingly, for the spin-polarized case, the spin states with antiferromagnetic or ferromagnetic ordering can be confined in a certain part of these structures. We also find that some partially open zigzag CNT superlattices are by themselves giant magnetoresistive devices. Moreover, the band gap as well as the energy of localized states of the superlattices could be tuned by external transverse electric fields, and bias voltages along the tube axis direction may be used to control the conductance of two different spin states. These properties may be useful for future device application in nanoelectronics.

V. ACKNOWLEDGMENTS

We gratefully acknowledge the supports by the KOSEF grant funded by MEST (Center for Nanotubes and Nanostructured Composites), the Korean Government MOEHRD, Basic Research Fund No. KRF-2006-341-C000015, the Core Competence Enhancement Program (2E2140) of KIST through the Hybrid Computational Science Laboratory (J.I.), a financial support (Grant No. KHU-20100119) from Kyung Hee University (G.K.), and KOSEF grant (Quantum Metamaterials research center, No. R11-2008-053-01002-0) funded by the MEST (Y.-W.S.). This work at China was supported by the Ministry of Science and Technology

of China (Grant Nos. 2006CB605105, 2006CB0L0601), and the National Natural Science Foundation of China (W.D, B.H., and Z.L.). B.H. also acknowledge the supports by the A3 Foresight Program of KOSEF-NSFC-JSPS. The computations were performed through the support of KISTI in Korea.

- ¹ A. K. Geim and K. S. Novoselov, *Nature Mater.* **6**, 183 (2007).
- ² A. H. Castro Neto, F. Guinea, N. M. R. Peres, K. S. Novoselov, and A. K. Geim, *Rev. Mod. Phys.* **81**, 109 (2009).
- ³ Charlier, J. C. Charlier, X. Blase, and S. Roche, *Rev. Mod. Phys.* **79**, 677 (2007).
- ⁴ P. Avouris, Z. Chen, and V. Perebeinos, *Nat. Nanotechnol.* **2**, 605 (2007).
- ⁵ S. J. Tans, A. R. M. Verschueren, and C. Dekker, *Nature* **393**, 49 (1998).
- ⁶ A. Javey, J. Guo, Q. Wang, M. Lundstrom, and H. Dai, *Nature* **424**, 654 (2003).
- ⁷ M. Fujita, K. Wakabayashi, K. Nakada, and K. Kusakabe, *J. Phys. Soc. Jpn.* **65**, 1920 (1996).
- ⁸ K. Nakada, M. Fujita, G. Dresselhaus, and M. S. Dresselhaus, *Phys. Rev. B* **54**, 17954 (1996).
- ⁹ K. Wakabayashi, M. Fujita, H. Ajiki, and M. Sigrist, *Phys. Rev. B* **59**, 8271 (1999).
- ¹⁰ Y. -W. Son, M. L. Cohen, and S. G. Louie, *Phys. Rev. Lett.* **97**, 216803 (2006).
- ¹¹ L. Chico, M. P. Lopez Sancho, and M. C. Munoz, *Phys. Rev. Lett.* **81**, 1278 (1998).
- ¹² Ç. Kılıç, S. Ciraci, O. Gülseren, and T. Yildirim, *Phys. Rev. B* **62**, R16345 (2000).
- ¹³ O. Gülseren, T. Yildirim, and S. Ciraci, *Phys. Rev. B* **68**, 115419 (2003).
- ¹⁴ L. Chico and W. Jaskolski, *Phys. Rev. B* **69**, 085406 (2004).
- ¹⁵ W. Zhang, W. Lu, and E. G. Wang, *Phys. Rev. B* **72**, 075438 (2005).
- ¹⁶ G. Kim, S. B. Lee, H. Lee and J. Ihm, *J. Phys.: Cond. Matt.* **19**, 26217 (2007).
- ¹⁷ B. Trauzettel, D. V. Bulaev, D. Loss, and G. Burlard, *Nat. Phys.* **3**, 3192 (2007).
- ¹⁸ J. Fernandez-Rossier and J. J. Palacios, *Phys. Rev. Lett.* **99**, 177204 (2007).
- ¹⁹ W. L. Wang, S. Meng, and E. Kaxiras, *Nano Lett.* **8**, 241 (2008).
- ²⁰ M. Topsakal, H. Sevincli, and S. Ciraci, *Appl. Phys. Lett.* **92**, 173118 (2008).
- ²¹ W. L. Wang, O. V. Yazyev, S. Meng, and E. Kaxiras, *Phys. Rev. Lett.* **102**, 157201 (2009).
- ²² A. D. Guclu, P. Potasz, O. Voznyy, M. Korkusinski, and P. Hawrylak, *Phys. Rev. Lett.* **103**, 246805 (2009).
- ²³ C. H. Park, L. Yang, Y. -W. Son, M. L. Cohen, and S. G. Louie, *Nat. Phys.* **4**, 213 (2008).

- ²⁴ H. Sevincli, M. Topsakal, and S. Ciraci, *Phys. Rev. B* **78**, 245402 (2008).
- ²⁵ C. H. Park, Y. -W. Son, L. Yang, M. L. Cohen, and S. G. Louie, *Phys. Rev. Lett.* **103**, 046808 (2009).
- ²⁶ M. Y. Han, B. Ozyilmaz, Y. Zhang, and P. Kim, *Phys. Rev. Lett.* **98**, 206805 (2007).
- ²⁷ Z. Chen, Y. M. Lin, M. J. Rooks, and P. Avouris, *Physica E* **40**, 228 (2007).
- ²⁸ L. Tapaszto, G. Dobrik, P. Lambin, and L. P. Biro, *Nat. Nanotechnol.* **3**, 397 (2008).
- ²⁹ X. Li, X. Wang, L. Zhang, S. Lee, and H. Dai, *Science* **319**, 1229 (2008).
- ³⁰ X. Yang, X. Dou, A. Rouhanipour, L. Zhi, H. J. Rader, and K. Mullen, *J. Am. Chem. Soc.* **130**, 4216 (2008).
- ³¹ D. V. Kosynkin, A. L. Higginbotham, A. Sinitskii, J. R. Lomeda, A. Dimiev, B. K. Price, and J. M. Tour, *Nature* **458**, 872 (2009).
- ³² Z. Zhang, Z. Sun, J. Yao, D. V. Kosynkin, and J. M. Tour, *J. Am. Chem. Soc.* **131**, 13460 (2009).
- ³³ L. Jiao, L. Zhang, X. Wang, G. Diankov, and H. Dai, *Nature* **458**, 877 (2009).
- ³⁴ A. G. Cano-Márquez, F. J. Rodríguez-Macias, J. Campos-Delgado, G. Espinosa-González, F. Tristán-Lopez, D. Ramírez-Gonzalez, D. A. Cullen, D. J. Smith, M. Terrones, and Y. Vega-Cantú, *Nano Lett.* **9**, 1527 (2009).
- ³⁵ A. L. Elías, A. R. Botello-Méndez, D. Meneses-Rodríguez, V. G. González, D. Ramírez-González, L. Ci, E. Munoz-Sandoval, P. M. Ajayan, H. Terrones, and M. Terrones, *Nano Lett.* **10**, 366 (2010).
- ³⁶ L. Jiao, X. Wang, G. Diankov, H. Wang, and H. Dai, *Nat. Nanotechnol.* DOI: 10.1038/NNANO.2010.54 (2010).
- ³⁷ L. Jiao, L. Zhang, L. Ding, J. Liu, and H. Dai, *Nano Res.* DOI: 10.1007/s12274-010-1043-z (2010).
- ³⁸ M. Terrones, *ACS Nano* **4**, 1775 (2010).
- ³⁹ B. Huang, F. Liu, J. Wu, B. -L. Gu, and W. H. Duan, *Phys. Rev. B* **77**, 153411 (2008).
- ⁴⁰ B. Huang, M. Liu, N. Su, J. Wu, W. H. Duan, B. -L. Gu, and F. Liu, *Phys. Rev. Lett.* **102**, 166404 (2009).
- ⁴¹ H. Santos, L. Chico, and L. Brey, *Phys. Rev. Lett.* **103**, 086801 (2009).
- ⁴² B. Huang, Y. -W. Son, G. Kim, W. H. Duan, and J. Ihm, *J. Am. Chem. Soc.* **131**, 17919 (2009).
- ⁴³ B. Wang, and J. Wang, *Phys. Rev. B* **81**, 045425 (2010).

- ⁴⁴ G. Kresse, and D. Joubert, Phys. Rev. B **59**, 1758 (1999).
- ⁴⁵ J. P. Perdew, K. Burke, and M. Ernzerhof, Phys. Rev. Lett. **77**, 3865 (1996).
- ⁴⁶ G. Kresse, and J. Furthmüller, Phys. Rev. B **54**, 11169 (1996).
- ⁴⁷ J. Neugebauer, and M. Scheffler, Phys. Rev. B **46**, 16067 (1992).
- ⁴⁸ N. L. Rangel, J. C. Sotelo, and J. M. Seminario, J. Chem. Phys. **131**, 031105 (2009).
- ⁴⁹ Z. Li, H. Qian, J. Wu, B.-L. Gu, and W. Duan, Phys. Rev. Lett. **100**, 206802 (2008).
- ⁵⁰ Y. -W. Son, M. L. Cohen, and S. G. Louie, Nature **444**, 347 (2006).
- ⁵¹ W. Y. Kim, and K. S. Kim, Nat. Nanotech. **3**, 408 (2008).
- ⁵² F. Munoz-Rojas, J. Fernandez-Rossier, and J. J. Palacios, Phys. Rev. Lett. **102**, 136810 (2009).
- ⁵³ S. Sahoo, T. Kontos, J. Furer, G. Hoffmann, M. Graber, A. Cottet, and C. Schonenberger, Nat. phys. **1**, 99 (2005).
- ⁵⁴ G. Fedorov, B. Lassagne, M. Sagnes, B. Raquet, J.-M. Broto, F. Triozon, S. Roche, and E. Flahaut, Phys. Rev. Lett. **94**, 066801 (2005).
- ⁵⁵ Y. -W. Son, J. Ihm, M. L. Cohen, S. G. Louie and H. J. Choi, Phys. Rev. Lett. **95**, 216602 (2005).
- ⁵⁶ Y. -W. Son, M. L. Cohen, and S. G. Louie, Nano Lett. **7**, 3518 (2007).
- ⁵⁷ L. G. Tien, C. H. Tsai, F. Y. Li, and M. H. Lee, Phys. Rev. B **72**, 245417 (2005).
- ⁵⁸ Z. Li, B. Huang, and W. Duan, J. Nanosci. Nanotechnol. **10**, 5374 (2010).